Article

A broadly applicable strategy for the fluorescence based detection and differentiation of glutathione and cysteine/ homocysteine: Demonstration in-vitro and in-vivo

Wenqiang Chen, Hongchen Luo, Xingjiang Liu, James Walter Foley, and Xiangzhi Song

Anal. Chem., **Just Accepted Manuscript** • DOI: 10.1021/acs.analchem.5b04333 • Publication Date (Web): 25 Feb 2016

A broadly applicable strategy for the fluorescence based detection and differentiation of glutathione and cysteine/homocysteine: Demonstration in-vitro and in-vivo

Wenqiang Chen,‡[a,b] Hongchen Luo,‡[a] Xingjiang Liu,[a] James W. Foley[c] and Xiangzhi Song*[a]

[a]College of Chemistry & Chemical Engineering, Central South University, 410083 Changsha, Hunan Province, P.R. China.

[b]College of Chemistry and Materials Science, Guangxi Teachers Education University, 530001 Nanning, Guangxi, P. R. China.

[c]Rowland Institute at Harvard , Harvard University, 02142, 100 Edwin H. Land Blvd. Cambridge, MA, USA.

*Corresponding author, Fax: +86-731-88836954; Tel: +86-731-88836954; E-mail: song@rowland.harvard.edu

ABSTRACT: Glutathione (GSH), cysteine (Cys) and homocysteine (Hcy) are small biomolecular thiols that are present in all cells and extracellular fluids of healthy mammals. It is well known that each plays a separate, critically important role in human physiology and that abnormal levels of each are predictive of a variety of different disease states. Although a number of fluorescence-based methods have been developed that can detect biomolecules that contain sulfhydryl moieties, few are able to differentiate between GSH and Cys/Hcy. In this report we demonstrate a broadly applicable approach for the design of fluorescent probes that can achieve this goal. The strategy we employ is to conjugate a fluorescence-quenching 7-nitro-2,1,3-benzoxadiazole (**NBD**) moiety to a selected fluorophore (Dye) through a sulfhydryl-labile ether linkage to afford nonfluorescent **NBD-O-Dye**. In the presence of GSH or Cys/Hcy, the ether bond is cleaved with the concomitant generation of both a nonfluorescent **NBD-S-R** derivative and a fluorescent dye having a characteristic intense emission band (**B1**). In the special case of Cys/Hcy, the **NBD-S-Cys/Hcy** cleavage product can undergo a further, rapid, intramolecular Smiles rearrangement to form a new, highly fluorescent **NBD-N-Cys/Hcy** compound (band **B2**); because of geometrical constraints, the GSH derived **NBD-S-GSH** derivative cannot undergo a Smiles rearrangement. Thus, the presence of a single **B1** or double **B1** + **B2** signature can be used to detect and differentiate GSH from Cys/Hcy, respectively. We demonstrate the broad applicability of our approach by including in our studies members of the Flavone, Bodipy and Coumarin dye families. Particularly, single excitation wavelength could be applied for the probe **NBD-OF** in the detection of GSH over Cys/Hcy in both aqueous solution and living cells.

INTRODUCTION SECTION

Sulfhydryl groups have many characteristics that have proven to be highly beneficial to mammals, plants and a variety of microscopic forms of life. The most prominent of these properties are the ability to (i) sequester inimical metal ions, (ii) inactivate reactive free radicals, (iii) quench reactive oxygen species and (iv) undergo reversible redox-mediated dimerization reactions.[1] Although evolutionary processes have produced a wide variety of thiol containing oligomers that are often unique to individual species, three specific small biomolecular thiols – glutathione (GSH), cysteine (Cys) and homocysteine (Hcy) – are present in all mammalian species as well as in some plants, bacteria and fungi.[2] Examples of the multiple roles each plays in mammalian physiology include: GSH, a mercaptotripeptide, functions as a detoxifying antioxidant that protects cells against damage caused by inimical heavy metals, peroxides and energetic free radicals as well as being an endogenous regulator of apoptosis.[3-4] Cys is a proteinogenic amino acid that confers structural integrity to proteins through the formation of crosslinking disulfide bonds and is also a precursor to GSH.[5] Hcy is a non-proteinogenic amino acid whose significance derives from its central role in three metabolic pathways (remethylation, transmethylation and transsulfuration) and, additionally, in mammals is a precursor of Cys.[6-7] Because of their ubiquity in mammals, especially humans, numerous studies have focused on establishing concentration levels of each in cells and in blood plasma that is required for good health. The findings of these studies indicate that abnormal levels of these biothiols are closely associated with a variety of health disorders including Alzheimer's and Parkinson's diseases, heart diseases, skin lesions, liver damage, cancer and HIV infection.[8-10] Recognition of the correlation each of these biothiols has with a particular subset of disease states has provided the incentive for researchers to develop methods to qualitatively and quantitatively measure both their presence and concentration in-vitro and in-vivo. Because of the sensitivity of fluorescence-based methodologies,[11] considerable effort has been expended in the development of probes that can detect and measure these physiologically important mercaptans. Several recent articles[12-20] devoted to this subject have noted that while a relative large number of innovative fluorescent probes have been discovered that can distinguish and measure sulfuryl containing biomolecules from other natural amino acids and their oligomers, few can distinguish GSH from Cys or Hcy.[18-27] While being of considerable value, most of the methods that can differentiate these three species are subject to a variety limitations including spectral

overlap between multiple emitting channels, slow response, or relatively poor selectivity.

In this report, we present a generic strategy for the design of fluorescent probes that can simultaneously detect and measure GSH in the absence and presence of Cys/Hcy and vice versa in vitro and in-vivo.

EXPERIMENTAL SECTION

Materials and Instruments: Unless otherwise noted, all reagents were obtained from commercial suppliers and used without further purification. Solvents were purified by standard methods prior to use. Twice-distilled water was used throughout all experiments. NMR spectra were recorded on a BRUKER 400/500 spectrometer with TMS as an internal standard. All accurate mass spectrometric experiments were performed on a micrOTOF-Q II mass spectrometer (Bruker Daltonik, Germany). UV-Vis absorption spectra were recorded on a Shimadzu UV-2450 spectrophotometer. Fluorescence spectra were recorded at room temperature using a HITACHI F-7000 fluorescence spectrophotometer with both the excitation and emission slit widths set at 5.0 nm. HPLC chromatograms were obtained using a Shimadzu LC-16 series instrument. TLC analysis was performed on silica gel plates and column chromatography was conducted using silica gel (mesh 200-300), both of which were obtained from Qingdao Ocean Chemicals, China.

Cell Culture and Fluorescence Imaging: HeLa cells were seeded in a 6-well plate in Dulbecco's modified Eagle's medium (DMEM) supplemented with 10% fetal bovine serum and 1% penicillin. The cells were incubated under an atmosphere of 5% CO2 and 95% air at 37°C for 24 h. Cell imaging was performed with a FV500 laser scanning confocal microscope. Before each experiment, cells were washed with PBS buffered solution 3 times. The cells were then incubated with NBD-OF (2.0 μM), or pretreated with GSH (1.0 mM, 30 min), Cys (1.0 mM, 30 min) or NEM (2.0 mM, 60 min) and further incubated with **NBD-OF** (2.0 μM) at 37 °C (for 60 min). Before the fluorescence imaging experiments were performed, cells were washed with PBS buffer 3 times. The samples were excited at 488 nm. Emission was collected at 510-535 nm (green channel) and 610-660 nm (red channel). With regard to **NBD-OBodipy**, similar experimental procedures were used except different excitation wavelengths were used (476 nm for green channel and 633 nm for red channel).

Synthesis of NBD-N-nBu: In a 5 mL round-bottom flask, 4-chloro-7-nitro-2,1,3-benzoxadiazole (**NBD-Cl**) (0.1 mmol, 20 mg) and n-butylamine (0.5 mmol, 50 μL) were dissolved in anhydrous acetonitrile (1 mL). The resulting mixture was stirred at room temperature for 2 h. The reaction mixture was poured into water (20 mL) and extracted with dichloromethane (2×20 mL). The organic layer was washed successively with water and brine, and dried over anhydrous Na_2SO_4 overnight. Following removal of the solvent, the crude product was purified by silica gel chromatography (DCM: PE = 1:1, v/v) to afford pure **NBD-N-nBu** as a brown solid (20 mg, 90%). ^{1}H NMR (500 MHz, $CDCl_3$) δ 8.50 (d, J = 8.6 Hz, 1H), 6.35 (s, 1H), 6.20 (d, J = 8.6 Hz, 1H), 3.53 (d, J = 5.8 Hz, 2H), 1.92 – 1.76 (m, 2H), 1.62 – 1.48 (m, 2H), 1.04 (t, J = 7.3 Hz, 3H). ^{13}C NMR (125 MHz, $CDCl_3$) δ 144.3, 144.0, 143.9, 136.6, 123.8, 98.6, 43.8, 30.5, 20.2, 13.7.

Synthesis of NBD-S-nPr: In a 5 mL round-bottom flask, **NBD-Cl** (0.1 mmol, 20 mg), 1-propanethiol (0.15 mmol, 11 mg) and trimethylamine (0.15 mmol, 20 μL) were dissolved in anhydrous acetonitrile (1 mL) and the resulting mixture was stirred at room temperature for 2 h. After removal of the solvent, the crude product was purified using column chromatography (silica gel; DCM: PE=1:1, v/v) to afford pure **NBD-S-nPr** as a yellow solid (13 mg, 56%). ^{1}H NMR (500 MHz, $CDCl_3$) δ 8.42 (d, J = 7.9 Hz, 1H), 7.17 (d, J = 7.9 Hz, 1H), 3.28 (t, J = 7.3 Hz, 2H), 1.92 (h, J = 7.3 Hz, 2H), 1.18 (t, J = 7.4 Hz, 3H). ^{13}C NMR (125 MHz, $CDCl_3$) δ 149.2, 142.5, 142.1, 132.5, 130.7, 120.2, 33.7, 21.5, 13.5.

Synthesis of compound NBD-OF: In a 5 mL round-bottom flask, compound **FOH**[28] (0.15 mmol, 45 mg), **NBD-Cl** (0.15 mmol, 30 mg) and trimethylamine (0.16 mmol, 22 μL) were dissolved in anhydrous acetonitrile (2 mL) and the resulting mixture was stirred overnight. The resulted precipitate was filtered and washed with cold ethanol (2×5 mL) and air-dried to afford pure **NBD-OF** as a brown solid (37 mg, 55%). ^{1}H NMR (500 MHz, DMSO-d_6) δ 8.61 (d, J = 8.4 Hz, 1H), 8.06 (dd, J = 7.9, 1.4 Hz, 1H), 7.93 – 7.81 (m, 3H), 7.60 (d, J = 8.9 Hz, 2H), 7.54 (t, J = 7.4 Hz, 1H), 7.16 (d, J = 8.4 Hz, 1H), 7.00 (d, J = 15.8 Hz, 1H), 6.71 (d, J = 9.0 Hz, 2H), 2.99 (s, 6H). ^{13}C NMR (125 MHz, DMSO-d_6) δ 170.1, 157.5, 155.2, 152.7, 152.4, 145.4, 144.83, 140.9, 138.2, 135.8, 134.9, 132.7, 131.0, 130.9, 125.8, 125.6, 124.1, 122.5, 118.8, 112.3, 111.4, 109.9, 107.8, 9.3. ESI-MS: $[M+H]^+$ calcd for 471.1299, found 471.1302.

Synthesis of compound NBD-OBodipy: In a 5 mL round-bottom flask, compound **Bodipy-OH** (0.04 mmol, 20 mg), **NBD-Cl** (0.04 mmol, 8 mg) and potassium carbonate (0.15 mmol, 21 mg) were dissolved in anhydrous acetone (2 mL) and the resulting mixture was stirred at room temperature for 4 h. After removal of the solvent, the residue was further purified by silica gel chromatography (DCM: PE=1:1, v/v) to afford pure **NBD-OBodipy** as a black solid (24 mg, 94%). ^{1}H NMR (500 MHz, $CDCl_3$) δ 8.53 (d, J = 8.3 Hz, 1H), 7.69 – 7.63 (m, 1H), 7.53 (d, J = 8.4 Hz, 2H), 7.41 (d, J = 8.4 Hz, 2H), 7.28 – 7.19 (m, 2H), 6.96 (t, J = 7.4 Hz, 1H), 6.89 (d, J = 14.6 Hz, 1H), 6.76 (d, J = 7.9 Hz, 1H), 6.63 (d, J = 8.3 Hz, 1H), 6.57 (s, 1H), 5.98 (s, 1H), 5.72 (d, J = 12.2 Hz, 1H), 3.24 (s, 3H), 2.59 (s, 3H), 1.65 (s, 5H), 1.58 (s, 3H), 1.50 (s, 3H). ^{13}C NMR (100 MHz, $CDCl_3$) δ 162.0, 156.6, 153.7, 153.2, 150.3, 145.2, 144.4, 144.1, 142.3, 139.2, 137.2, 136.8, 135.0, 133.7, 133.5, 133.2, 131.6, 131.3, 131.1, 130.4, 128.4, 128.0, 121.6, 121.3, 120.9, 119.8, 118.4, 113.6, 108.0, 107.0, 98.5, 46.6, 46.4, 29.6, 29.3, 28.7, 15.0, 14.2. ESI-MS: $[M+H]^+$ calcd for 687.2697, found 687.2706.

Synthesis of compound NBD-OCoumarin:[29] In a 10 mL round-bottom flask, compound Coumarin-OH (0.15 mmol, 27 mg), **NBD-Cl** (0.15 mmol, 30 mg) and trimethylamine (0.32 mmol, 44 μL) were dissolved in anhydrous ethanol (3 mL) and the resulting mixture was stirred at room temperature for 8 h. The resulted precipitate was filtered, washed with cold methanol (2×4 mL) and air-dried to afford pure **NBD-OCoumarin** as brown solid (32 mg, 60%). ^{1}H NMR (400 MHz, DMSO-d_6) δ 8.67 (d, J = 8.3 Hz, 1H), 7.99 (d, J = 8.7 Hz, 1H), 7.57 (d, J = 2.4 Hz, 1H), 7.45 (dd, J = 8.7, 2.4 Hz, 1H), 7.00 (d, J = 8.3 Hz, 1H), 6.47 (s, 1H), 2.49 (s, 3H). ^{13}C NMR (100 MHz, DMSO-d6) δ 159.9, 156.1, 154.7, 153.4, 152.3, 145.9, 144.9, 135.6, 131.6, 128.3, 118.6, 117.2, 114.5, 112.3, 109.2, 18.7.

RESULTS AND DISCUSSION

The strategy we used to design fluorescent probes for the simultaneous detection and quantitation of GSH and Cys/Hcy, as depicted in Scheme 1, was based on well-established concepts and experimental observations. Most important among these were: (1) Sulfhydryl groups (more polarizable) are both (i) more nucleophilic and (ii) better S_NAr leaving groups than are amino moieties (less polarizable);[30-31] (2) In physiological conditions (pH=7.4), the thiols are ionized, while the amino groups are protonated. As a result, 4-aryloxy-7-nitro-2,1,3-benzoxadia-zoles (**NBD-OAr**) are susceptible to S_NAr substitution by sulfhydryl alkanes but are resistant to attack by amino alkanes under this condition; (3) Intramolecular rearrangements involving 5 and 6 membered rings are kinetically strongly favored over those involving larger ring systems;[32] (4) Fluorescence efficiency of 4-substituted-7-nitro-2,1,3-benzoxadiazoles (**NBD-X**) markedly depends on the electron-donating ability of X through effective ICT process (e.g. relative fluorescence quantum yields in methanol: X = $NHCH_3$: 62.7; SCH_3: 0.6; OCH_3, 0.0);[33] (5) 7-Nitro-2,1,3-benzoxadiazole (**NBD**) can efficiently quench the fluorescence of a variety of dyes via a strong photoinduced electron transfer (PET) process.

Scheme 1. Proposed mechanism for the discriminative detection of GSH and Cys/Hcy for NBD-based fluorescent probes.

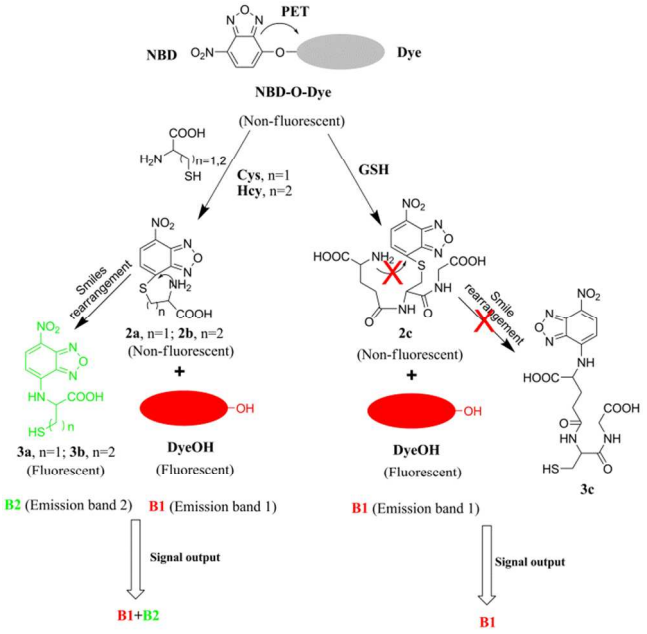

With this knowledge in mind, we reasoned that conjugating an **NBD** group to the OH moiety of a hydroxyl-substituted fluorescent dye (**DyeOH**) would result in the formation of a nonfluorescent **NBD-O-Dye**. As noted above, in aqueous environments the ether linkage of this type of conjugate should be impervious to attack by amino nucleophiles, such as those found in typical amino acids. Contrariwise, treatment of **NBD-O-Dye** with a biothiol, such as a sulfhydryl containing amino acid, was expected to rapidly cleave the ether bond via a bimolecular S_NAr mechanism to afford **NBD-SR** and **DyeOH**; such a reaction would be accompanied by the formation of a single, highly fluorescence emission band (**B1**) corresponding to that of the untethered dye. In the special case where the biothiol also contains a suitably situated amino moiety, as is the case for amino acids Cys and Hcy, the initially formed displacement product, **NBD-S-Cys/Hcy(2a/2b)**, can undergo a further, rapid Smiles rearrangement to give **NBD-N-Cys/Hcy(3a/3b)** via a 5- or 6-member cyclic intermediate, respectively. Such a transformation would be accompanied by the formation of a second, intense emission band (**B2**) corresponding to that of **NBD-NHR**. We note that we would expect amino-biothiols such as GSH to participate in the initial S_NAr displacement reaction with **NBD-O-Dye** but not in the subsequent Smiles rearrangement because to do so would require the intervention of a 10-member cyclic transition state. Consequently, the signature of such a reaction would be the formation of only a **B1** band. In summary, with the expectation that the only significant amino-biothiols that would normally be encountered in mammalian cells and blood are GSH, Cys and Hcy, treatment of either cells or plasma with **NBD-O-Dye** would give (i) no fluorescence signal in the absence of all three, (ii) a single **B1** band if only GSH was present, and (iii) dual **B1** + **B2** signals with prescribed relative intensities if only Cys and/or Hcy were present; intermediate **B1** + **B2** relative band intensities should, upon deconvolution, give the ratio of GSH to Cys/Hcy.

Scheme 2. Synthetic route to NBD-OF and chemical structure of control compounds NBD-N-NBu and NBD-S-nPr.

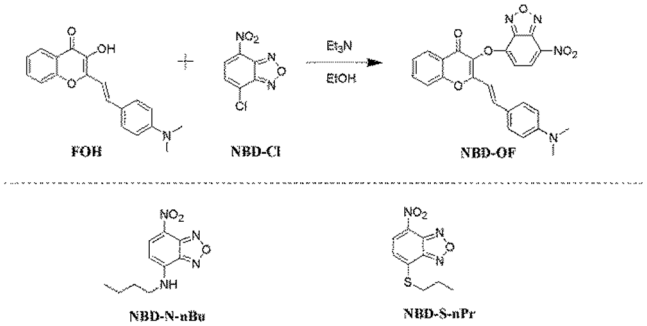

In order to demonstrate a proof-of-concept, we initially synthesized **NBD-OF** wherein starting material **FOH** our previously reported long wavelength 3-hydroxyflavone derivative (Scheme 2).[28] The selection of **FOH** as a **NBD**-quenchable dye was based on the following considerations: (1) **FOH** displays many favorable optical properties such as large Stokes shift, good photostability, and strong fluorescence in red spectral region; (2) The absorption spectra of **FOH** and **NBD-N-nBu** (455 nm for **FOH**, and 476 nm for **NBD-N-nBu**) (Figure S2) were largely overlapped in PBS buffer (10.0 mM, pH 7.4, containing 30% CH_3CN, v/v), which enabled the simultaneous excitation of both chromophores by a single excitation band, which can simplify multi-channel fluorescence microscopy experiments.

The time-dependent fluorescence measurements of **NBD-OF** toward Cys/Hcy/GSH were performed in PBS buffer (10.0 mM, pH 7.4, containing 30% CH_3CN, v/v). As shown in Figure 1, **NBD-OF** was observed to be essentially non-fluorescent due to the efficient PET process induced by the **NBD** moiety. Upon the addition of either Cys or Hcy, the formation of two emission bands centered at 545 nm and 621 nm were immediately observed, having nearly identical wavelengths and band shapes expected for **FOH** and control compound **NBD-N-nBu**, respectively. Both emission bands increased as a function of time, levelling off after approximately 60 min (Figure 1), and the pseudo-first-order rate constants for Cys and Hcy were calculate to be 5.56×10^{-2} min^{-1}, 2.82×10^{-2} min^{-1}, respectively (Figure S4-S5). This behavior was consistent with what was expected if Cys/Hcy had cleaved the

ether bond in **NBD-OF**, releasing the fluorescent **FOH** (λ_{max}em = 621 nm) and the corresponding intermediates **NBD-S-Cys/Hcy**, **2a**/**2b**, which subsequently was transformed into fluorescent **NBD-N-Cys/Hcy**, **3a**/**3b** (λ_{max}em = 545 nm) (Figure S3). On the other hand, treatment of **NBD-OF** with GSH, produced only a single intense fluorescence band with λ_{max}em = 621 nm and a negligible fluorescence signal at λ_{max}em = 545 nm, suggesting that GSH induced a S_NAr thiolysis of **NBD-OF** to afford fluorescent **FOH** and the non-fluorescent intermediate **2c** (Figure 1). Separately, we found that **NBD-OF** was capable of discriminating Cys/Hcy from GSH simply by using the naked eye to observe under the illumination of a UV 365 nm lamp (Figure 2). It is readily apparent that introduction of Cys/Hcy to a solution of **NBD-OF** elicited a strong orange emission. In contrast, the addition of GSH to a separate solution of **NBD-OF** resulted in the emission of bright red photons. We note that in order to ensure the expected generic **NBD-SR** cleavage product produced an insignificant fluorescence signal in our solvent system (30% acetonitrile/70% water), we prepared control compound, **NBD-S-nPr** and found that, in deed, its behavior mirrored that reported for **NBD-SCH$_3$** in methanol (vide supra). These experiments provide strong support for the generic idea that **NBD-O-Dye** has the potential to act as a fluorescent probe for the simultaneous detection of GSH and Cys/Hcy.

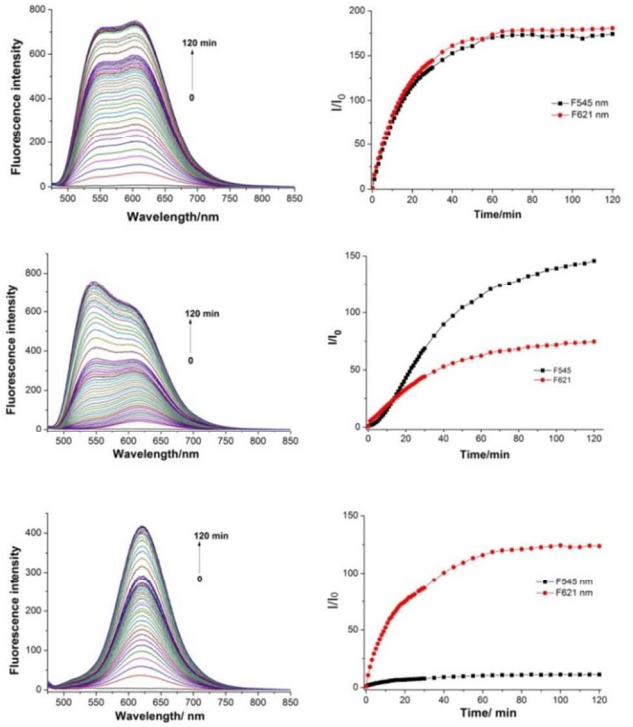

Figure 1. Time-dependent fluorescence of **NBD-OF** (5.0 μM) with 100 equiv. of Cys (A1, A2), Hcy (B1, B2) and GSH (C1, C2) in PBS buffer (10.0 mM, pH 7.4, containing 30% CH_3CN, v/v). Excited at 458 nm.

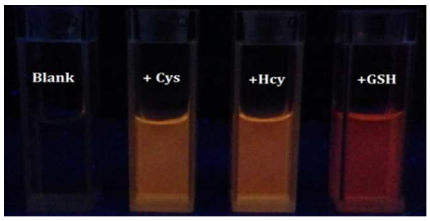

Figure 2. Fluorescence images of **NBD-OF** alone and in the presence of GSH, Cys and Hcy under illumination by a UV 365 lamp.

The fluorescence of **NBD-OF** in response to different concentrations of Cys, Hcy and GSH were investigated in PBS buffer (10.0 mM, pH 7.4, containing 30% CH_3CN, v/v). For Cys/Hcy, the fluorescence intensity was linearly related to the concentrations Cys/Hcy in the range of 0.0-500.0 μM (Figure S7-S10). The detection limits for Cys and Hcy were calculated to be 2.1×10^{-6} M and 2.7×10^{-6} M, respectively base on S/N = 3. In the case of GSH, the fluorescence intensity at 621 nm was linear with the concentration of GSH in the range of 0.0-600.0 μM (Figure S11-S12); the detection limit was determined to be 6.4×10^{-6} M based on S/N = 3. Moreover, we investigated the fluorescence behavior of **NBD-OF** (5.0μM) treated with 50 equiv. of GSH in the presence of different concentrations (0.0 μM, 25.0 μM, 50.0 μM and 75.0 μM) of Cys in PBS buffer (10.0 mM, pH 7.4, containing 30% CH_3CN, v/v). After incubation the mixture for 2 hours, the addition of 50 equiv. of GSH only induced a significant fluorescence signal with a peak at 621 nm. However, the addition of Cys and GSH induced the fluorescence enhancement at both 621 nm and 545 nm. It is noteworthy that the fluorescence intensity at 545 nm was linearly proportional to the concentration of Cys (Figure S13-S14). The results indicated that **NBD-OF** could detect Cys in the presence of GSH.

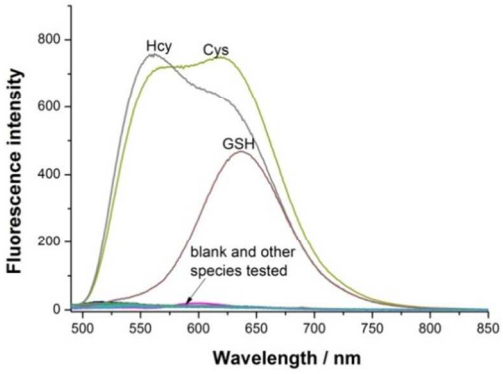

Figure 3. Fluorescence spectra of **NBD-OF** upon the addition of 100.0 equiv. of various biological species: Cys, Hcy, GSH, Ala, Arg, Asp, Gln, Glu, His, Ile, Leu, Lys, Met, Phe, Pro, Ser, Thr, Try, Tyr, Val, GSH and ascorbic acid in PBS buffer (10.0 mM, pH 7.4, containing 30% CH_3CN, v/v). Each spectrum was recorded after the addition of the corresponding species for 120 min.

To evaluate the selectivity of **NBD-OF** toward GSH and Cys/Hcy over various relevant biomolecules, we examined the fluorescence of **NBD-OF** in response to amino acids Cys, Hcy, His, Glu, Asp, Val, Phe, Tyr, Ala, Ser, Leu, Arg, Pro, Thr, Gln, Try, Ile, Lys as well as with GSH and ascorbic acid

(Figure 3). The findings of this evaluation were that of this entire array of biomolecules, only GSH and Cys/Hcy induced a significant fluorescence response. Thus, **NBD-OF** appears to be a highly selective probe for GSH and Cys/Hcy.

To determine whether **NBD-OF** can function under physiological conditions, we studied its response toward GSH and Cys/Hcy as a function of pH. As is evident from inspection of the data presented in Figure 4, in the absence of biothiols, **NBD-OF** is very stable over the physiological relevant pH range of 2-10. Importantly, **NBD-OF** displays a strong fluorescence enhancement in the presence of the biothiols of the present study in the pH range of 7-8 which suggests that it can function under physiological conditions.

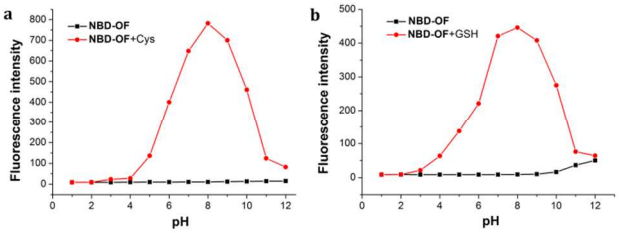

Figure 4. pH effect on the fluorescence intensity of **NBD-OF** (5.0 μM) in absence and presence of 100.0 equiv. of Cys (λ_{em} = 545 nm) (a) and GSH (λ_{em} = 621 nm) (b). Sample intensity at each pH was measured after 120 min.

To demonstrate the broad applicability of our strategy for designing fluorescent probes for simultaneous detection GSH and Cys/Hcy, we developed another probe: **NBD-OBodipy** (Scheme 3). The Bodipy derivative has an absorption maximum at 650 nm and fluorescence in near infrared region with λ_{max} = 705 nm. As shown in Figures 5a and S15, the addition of 10.0 equiv. of Cys/Hcy/GSH to **NBD-OBodipy** induced a strong fluorescence **B1** band centered at 705 nm (at 120 minutes a 726-fold increase in intensity for Cys, 709-fold for Hcy and 720-fold for GSH). The significant fluorescence enhancement in the NIR region renders **NBD-OBodipy** especially suitable for in vivo applications because NIR light can minimized photodamage to biological samples, has better tissue penetration than visible photons and has less interference from background autofluorescence commonly encountered in living systems.[34] Moreover, the addition of Cys/Hcy triggered an additional fluorescence **B2** band at 545 nm (70-fold intensity enhancement for Cys and 80-fold for Hcy) when excited at 476 nm (Figures 5b and S16). By sharp contrast, emission at 545 nm was negligible when **NBD-OBodipy** was treated with GSH. As expected, **NBD-OBodipy** was able to discriminate of Cys/Hcy from GSH by the presence or absence of a **B2** band at 545 nm.

In order to evaluate its selectivity, the fluorescence behaviours of **NBD-OBodipy** toward other biologically relevant amino acids were investigated. As illustrated in Figure 5, no significant fluorescence response was generate by a series of biologically relevant amino acids whereas Cys, Hcy and GSH induced a significant fluorescence band at 705 nm when excited at 650 nm. In addition, with the exception of Cys and Hcy, none of the tested chemicals, including GSH, produced significant emission at 545 nm when excited at 476 nm. These results demonstrate that **NBD-OBodipy** is highly selective for the detection and discrimination of GSH from Cys/Hcy and all three of these biothiols from a wide array of common amino acids.

Scheme 3. Structures of NBD-OBodipy and NBD-OCoumarin.

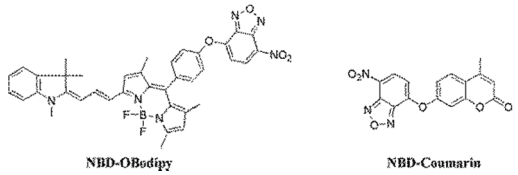

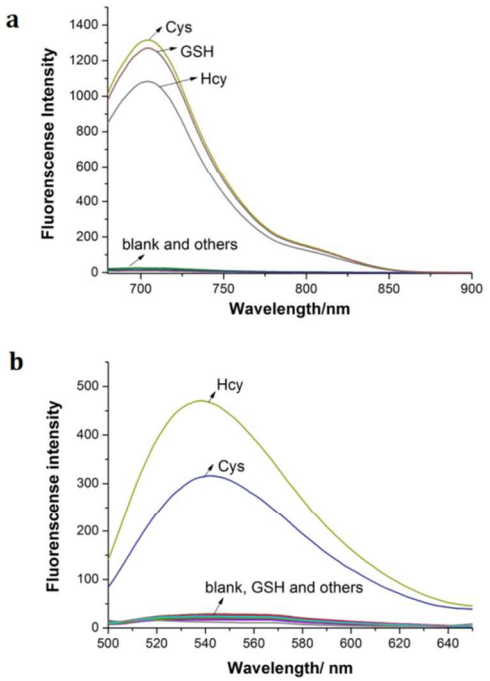

Figure 5. Fluorescence spectra of **NBD-OBodipy** (5.0 μM) upon the addition of various amino acids in PBS buffer (10.0 mM, pH 7.4, containing 1.0 mM CTAB) at room temperature. (a) Excited at 650 nm; (b) Excited at 476 nm. Each spectrum was recorded 120 min after incubation with corresponding species. Amino acid: Cys, Hcy, GSH, Ala, Gln, Glu, His, Ile, Leu, Lys, Phe, Pro, Ser, Thr, Try, Tyr, Val.

Pluth and co-workers have reported a coumarin-based fluorescent probe, **NBD-OCoumarin**, to discriminate H_2S from Cys/Hcy employing **NBD** moiety as the sensing group.[29] Indeed, **NBD-OCoumarin** in Pluth's work also has the ability to discrimination GSH from Cys/Hcy. We synthesized **NBD-OCoumarin** and studied its fluorescence behavior in response to biothiols. The addition of Cys, Hcy or GSH to **NBD-OCoumarin** in PBS buffer (10 mM, pH 7.4, containing 30% CH_3CN, v/v) caused a significant fluorescence band to appear at 445 nm when excited at 380 nm, reaching a maximum within 10 min (Figure S17). Moreover, Cys/Hcy induced a fluorescence band at 545 nm when excited at 476 nm. Due to the large difference in their absorption spectra between **Coumarin-OH** and **3a/3b**, **NBD-OCoumarin** was unable to work with single excitation wavelength for the discrimination of GSH from Cys/Hcy with naked eye. On the contrary, the absorption spectral overlap between the resulting fluorescent fragments **FOH** and **3a/3b** from **NBD-OF** is large and the simultaneous excitation of both chromophores by a single excitation band can be achieved, which can simplify multichannel fluorescence microscopy experiments. Moreover, the

emission of **FOH** is in red spectral region, which is desirable for biological fluorescence detection due to the deeper penetration in biological tissues. Also, the intensities of two fluorescence signal from **FOH** and **3a**/**3b** generated from **NBD-OF** in PBS buffer are quite comparable when excited at 458 nm, which is desirable for the discriminatory detection.

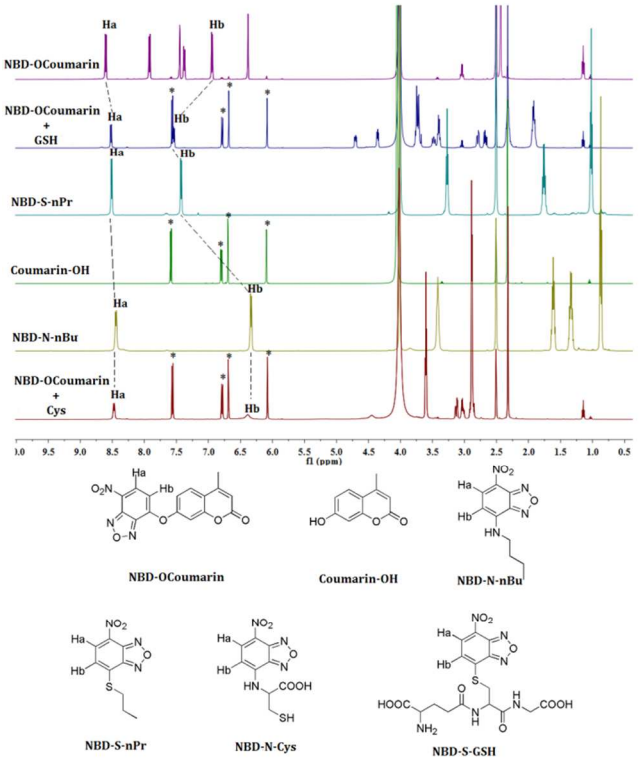

Figure 6. ^{1}H NMR spectral comparison of **NBD-OCoumarin**, **Coumarin-OH**, **NBD-N-nBu**, **NBD-S-nPr**, **NBD-OCoumarin** with Cys and GSH. All ^{1}H NMR spectra were obtained in DMSO-d_6-D_2O (4:1, v/v).

To provide data supporting for our proposed mechanism of action, we performed ^{1}H NMR titration experiments designed to follow product formation resulting from the cleavage and possible subsequent Smiles rearrangement of our probes. Compound **NBD-OCoumarin** was utilized to perform this experiment due to its good solubility in solution. Upon the addition of excessive Cys or GSH to **NBD-OCoumarin** in DMSO-d_6-D_2O (4:1, v/v), signals corresponding to each of the protons attributable to **Coumarin-OH** began to appear, indicating the release of **Coumarin-OH** whereas the proton signals associated with **NBD** depended on whether the biothiol reactant was Cys or GSH. When Cys was the reactant, the Ha and Hb protons of the **NBD** moiety showed upfield shifts, especially for Hb, which were expected if **NBD-NHR** was being formed. However, when GSH was the reactant, the growing signals for the Ha and Hb protons of **NBD** had chemical shifts that corresponded with those expected for **NBD-SR**. HPLC is an effective method widely used in the separation and analysis of mixtures of organic compounds. Thus, **NBD-OCoumarin**, the reference dye **Coumarin-OH** and the reaction mixture of **NBD-OCoumarin** with Cys, Hcy and GSH were subjected to HPLC analysis (Figure S18-S20). **NBD-OCoumarin** itself displayed a single peak with a retention time at 11.07 min. **Coumarin-OH** displayed a single peak with a retention time at 6.06 min. With the addition of the incremental amounts of Cys, the peak of **NBD-OCoumarin** was gradually disappeared; two new peaks were emerged with the retention times at 3.90 min, which is assigned to compound **3a**, and 6.06 min, which is assigned to **Coumarin-OH** (Figure S18). Similar results were obtained for the reaction mixture of **NBD-OCoumarin** with Hcy and GSH and the retention times of compounds **3b** and **2c** were found to be 3.84 min and 3.67 min, respectively (Figure S19-S20). Additionally, HRMS analysis of the reaction mixture of **NBD-OCoumarin** with Cys, Hcy and GSH confirmed the formation of **Coumarin-OH** (*m/z* = 199.0387, $[M+Na]^+$) and other fragments (*m/z* = 307.0153 for **3a**, $[M+Na]^+$; 299.0449 for **3b**, $[M+1]^+$; and 493.0768 for **2c**, $[M+Na]^+$) (Figure S21-S23). These results provided strong support for our proposal that GSH and Cys/Hcy both induce thiolysis to release **Coumarin-OH** but that only the **NBD-SR** compound derived from Cys/Hcy has the ability to undergo a subsequent Smiles rearrangement to form **NBD-NHR**.

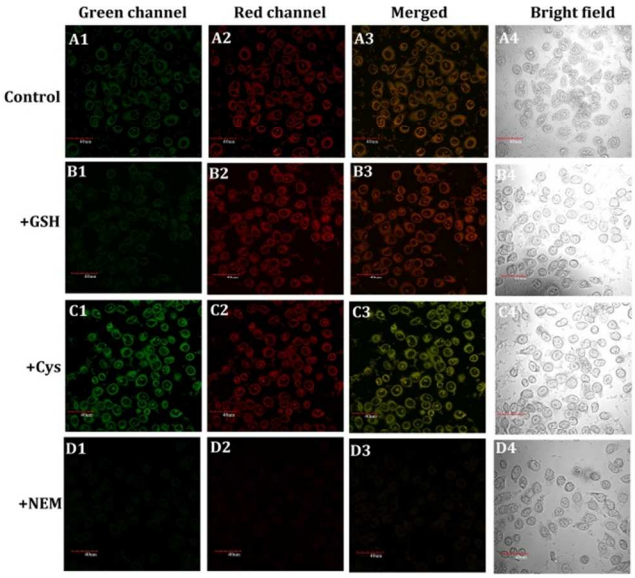

Figure 7. Confocal microscopic images of Cys and GSH in HeLa cells. (A1-A4) HeLa cells incubated with 2.0 μM **NBD-OF**. (B1-B4) HeLa cells pre-treated with 1.0 mM GSH and then incubated with 2.0 μM **NBD-OF**. (C1-C4) HeLa cells pre-treated with 1.0 mM Cys and then incubated with 2.0 μM **NBD-OF**. (D1-D4) HeLa cells pre-treated with 1.0 mM NEM and then incubated with 2.0 μM **NBD-OF**. Excitation wavelength: 488 nm. Emission was collected at 510-535 nm for green channel and 610-660 nm for red channel. Scale bar: 40 μm.

Encouraged by the aforementioned results, we evaluated the capability of **NBD-OF** to selectively image intracellular Cys and GSH with the aid of confocal microscopy. The microscope was fitted with both green and red light detection optics which correspond to the emitted photons from **NBD-NHR** and **FOH**, respectively; a single excitation band centered at 488 nm was used to excite both chromophores. When HeLa cells were incubated with **NBD-OF** (2.0 μM), the fluorescence signals from green and red channels were observed (Figure 7 A1-A4). For the control experiment, HeLa cells were incubated with either Cys (1.0 mM) or GSH (1.0 mM) and, after changing the growth medium, were incubated with **NBD-OF** (2.0 μM) whereupon the fluorescence signals from the green

and red channels were recorded and viewed either separately or merged together (Figure 7 B1-B4 and C1-C4). As a control, a batch of cells initially treated with 2.0 mM N-ethylmaleimide (NEM) to inactivate all intracellular thiol species and then incubated with 2.0 μM **NBD-OF** showed faint fluorescence signals in green and red channels (Figure 7 D1-D4). Inspection of Figure 7 shows that cells treated with GSH glowed bright red and but were nearly devoid of signal in the green channel. In sharp contrast, cells treated with Cys exhibited strong fluorescence images in both the red and green channels which, when merged, produced bright yellow images. The NEM treated control cells did not generate significant images in either the red or green channels. Taken together, these experiments show that **NBD-OF** can interact with biothiols under intracellular physiological conditions in the same manner as it does in-vitro. Therefore, **NBD-OF** has the potential to be an in-vivo probe for the detection and differentiation of Cys and GSH with a single excitation wavelength.

Moreover, we utilized the NIR probe, **NBD-OBodipy**, to image intracellular Cys and GSH in living HeLa cells. As shown in Figure S24, similar results were obtained that bright yellow signal, merged from the red and green channels, was observed inside the cells. In contrast, cells treated with GSH only exhibited strong red fluorescence. These results suggest that **NBD-OBodipy** is capable of imaging intracellular Cys and GSH from different emission channel.

CONCLUSIONS

In conclusion, we have developed a broadly approach to designing fluorescent probes for simultaneous detection of GSH and Cys/Hcy both in-vivo and in-vitro. The strategy is based on selective thiolysis and intramolecular rearrangement reactions when NBD is conjugated to light-induced electron donating dyes through a labile ether linkage. As a proof-of-concept, we have explored three novel fluorescent probes, **NBD-OF**, **NBD-OBodipy** and **NBD-OCoumarin**, which can discriminate GSH from Cys/Hcy and all three from a wide array of amino acids with good selectivity and sensitivity. Moreover, we also demonstrated that probes, **NBD-OF**, **NBD-OBodipy**, were capable of simultaneously imaging intracellular GSH and Cys in living cells. This novel strategy reported herein has the potential to inspire the development of new fluorescent probes with desired properties for the discriminatory detection of GSH and Cys/Hcy.

ASSOCIATED CONTENT

Supporting Information

Chemical structures of compounds, additional spectra data, confocal microscopy images, ^{1}H, ^{13}C and HRMS spectra of compounds. The Supporting Information is available free of charge via the Intenet at http://pubs.acs.org.

AUTHOR INFORMATION

Corresponding Author

*E-mail: song@rowland.harvard.edu

Author Contributions

‡These authors contributed equally to this work.

Notes

The authors declare no competing financial interest.

ACKNOWLEDGMENT

This research was supported by the State Key Laboratory of Fine Chemicals (KF1202) and the State Key Laboratory for Powder Metallurgy.

REFERENCES

1 Patai, S.; Rappoport, Z. *Sulphur-Containing Functional Groups*; John Wiley & Sons Inc.: Chichester, **1993**.
2 Ingenbleek, Y. *J. Nutr.* 2006, 136, 16415.
3 Chen, X.; Tian, X.; Shin, I.; Yoon, J. *Chem. Soc. Rev.* **2011**, 40, 4783-4804.
4 Meister, A.; Anderson, M. E. *Annu. Rev. Biochem.* **1983**, 52, 711-760.
5 Weerapana, E.; Wang, C. G. M. Simon, G. M.; Richter, F.; Khare, S.; Dillon, M. B. D.; Bachovchin, D. A.; Mowen, K.; Baker, D.; Cravatt, B. F. *Nature* **2010**, 468, 790-795.
6 Finkelstein, J. D. *Eur. J. Pediatr.* **1998**, 157, S40-S44.
7 Hultberg, B.; Andersson, A.; Isaksson, A. *Toxicology* **1997**, 123, 33-40.
8 Seshadri, S.; Beiser, A.; Selhub, J.; Jacques, P. E.; Rosenberg, I. H.; D'Agostino, R. B.; Wilson, P. W. F.; Wolf, P. A. *N. Engl. J. Med.* **2002**, 346, 476-483.
9 Shahrokhian, S. *Anal. Chem.* **2001**, 73, 5972-5978.
10 Townsend, D. M.; Tew, K. D.; Tapiero, H. *Biomed. Pharmacother.* **2003**, 57, 145-155.
11 Yang, Y.; Zhao, Q.; Feng, W.; Li, F. *Chem. Rev.* **2013**, 113, 192-270.
12 Jung, H. S.; Chen, X.; Kim J. S.; Yoon, J. *Chem. Soc. Rev.* **2013**, 42, 6019-6031.
13 Manjare, S. T.; Kim, Y.; Churchill, D. G. *Acc. Chem. Res.* **2014**, 47, 2985-2998.
14 Yin, C.; Huo, F.; Zhang, J.; Martinez-Manez, Y.; Yang, H. L.; Li, S. *Chem. Soc. Rev.* **2013**, 42, 6032-6059.
15 Zhou, Y.; Yoon, J. *Chem. Soc. Rev.* **2012**, 41, 52-67.
16 Niu, L. Y.; Chen, Y. Z.; Zheng, H. R.; Wu, L. Z.; Tung, C. H.; Yang, Q. Z. *Chem. Soc. Rev.* **2015**, 44, 6143-6160.
17 Wang, F.; An, J.; Zhang, L.; Zhao, C. *RSC Adv.* **2014**, 4, 53437-53441.
18 Wang, F.; Guo, Z.; Li, X.; Li, X.; Zhao, C. *Chem. Eur. J.* **2014**, 20, 11471-11478.
19 Zhao, C.; Li, X.; Wang, F. *Chem. –Asian. J.* **2014**, 9, 1777-1781.
20 Zhao, C.; Zhang, X.; Li, B.; Zhu, S.; Guo, Z.; Zhang, L.; Wang, F.; Fei, Q.; Luo, S.; Shi, P.; Tian, H.; Zhu, W. *J. Am. Chem. Soc.* **2015**, 137, 8490-8498.
21 Yang, X. F.; Huang, Q.; Zhong, Y.; Li, Z.; Li, H.; Lowry, M.; Escobedo, J. O.; Strongin, R. M. *Chem. Sci.* **2014**, 5, 2177-2183.
22 Zhang, Y.; Shao, X.; Wang, Y.; Pan, F.; Kang, R.; Peng, F.; Huang, Z.; Zhang, W.; Zhao, W. *Chem. Comm.* **2015**, 51, 4245-4248.
23 Liu, J.; Sun, Y. Q.; Zhang, H.; Huo, Y.; Shi, Y.; Guo, W. *Chem. Sci.* **2014**, 5, 3183-3188.
24 Liu, J.; Sun, Y.-Q.; Huo, Y.; Zhang, H.; Wang, L.; Zhang, P.; Song, D.; Shi, Y.; Guo, W. *J. Am. Chem. Soc.* **2014**, 136, 574-577.
25 Wang, F.; Zhou, L.; Zhao, C.; Wang, R.; Fei, Q.; Luo, S.; Guo, Z.; Tian, H.; Zhu, W. H. *Chem. Sci.* **2015**, 6, 2584-2589.
26 Zhang, H.; Liu, R.; Liu, J.; Li, L.; Wang, P.; Yao, S. Q.; Xu, Z.; Sun, H. *Chem. Sci.* **2016**, 7, 256-260.
27 Kim, Y.; Mulay, S. V.; Choi, M. ;Yu, S. B. ;Jon, S. ;Churchill, D. G. *Chem. Sci.* **2015**, 6, 5435-5439.
28 Chen, S.; Hou, P.; Zhou, B.; Song, X.; Wu, J.; Zhang, H.; Foley, J. W. *RSC Adv.* **2013**, 3, 11543-11546.
29 Hammers, M. D.; Pluth, M. D. *Anal. Chem.* **2014**, 86, 7135-7140.
30 Friedman, M.; Cavinsand, J. F.; Wall, J. S. *J. Am. Chem. Soc.* **1965**, 87, 3672-3682.
31 Singh, R.; Whitesides, G. M. *In Sulphur-Containing Functional Groups*; Patai, S.; Rappoport, Z. Ed.; John Wiley & Sons Inc.: Chichester, **1993**; 633-658.

32 Niu, L. Y.; Guan, Y. S.; Chen, Y. Z.; Wu, L. Z.; Tung, C. H.; Yang, Q. Z. *J. Am. Chem. Soc.* **2012**, 134, 18928-18931.
33 Uchiyama, S.; Santa, T.; Fukushima, T.; Homma, H.; Imai, K. *J. Chem. Soc. Perkin Trans.* **1998**, 2, 2165-2174.
34 Yuan, L.; Lin, W.; Zheng, K.; He, L.; Huang, W.; *Chem. Soc. Rev.* **2013**, 42, 622-661.

for TOC only